Saccharomyces cerevisiae Vacuole in Zinc Storage and Intracellular Zinc Distribution[▽][‡]

Claudia Simm,[1]† Brett Lahner,[2] David Salt,[2] Ann LeFurgey,[3] Peter Ingram,[4]
Brian Yandell,[5] and David J. Eide[1]*

*Department of Nutritional Sciences, University of Wisconsin—Madison, Madison, Wisconsin 53706[1]; Department of
Horticulture and Landscape Architecture, Purdue University, West Lafayette, Indiana 47907-2010[2]; Department of
Cell Biology, Duke University Medical Center and Veterans Affairs Medical Center, Durham, North Carolina 27705[3];
Department of Pathology, Duke University Medical Center, Durham, North Carolina 27710[4]; and Departments of
Statistics and Horticulture, University of Wisconsin—Madison, Madison, Wisconsin 53706[5]*

Previous studies of the yeast *Saccharomyces cerevisiae* indicated that the vacuole is a major site of zinc storage in the cell. However, these studies did not address the absolute level of zinc that was stored in the vacuole nor did they examine the abundances of stored zinc in other compartments of the cell. In this report, we describe an analysis of the cellular distribution of zinc by use of both an organellar fractionation method and an electron probe X-ray microanalysis. With these methods, we determined that zinc levels in the vacuole vary with zinc status and can rise to almost 100 mM zinc (i.e., 7×10^8 atoms of vacuolar zinc per cell). Moreover, this zinc can be mobilized effectively to supply the needs of as many as eight generations of progeny cells under zinc starvation conditions. While the Zrc1 and Cot1 zinc transporters are essential for zinc uptake into the vacuole under steady-state growth conditions, additional transporters help mediate zinc uptake into the vacuole during "zinc shock," when zinc-limited cells are resupplied with zinc. In addition, we found that other compartments of the cell do not provide significant stores of zinc. In particular, zinc accumulation in mitochondria is low and is homeostatically regulated independently of vacuolar zinc storage. Finally, we observed a strong correlation between zinc status and the levels of magnesium and phosphorus accumulated in cells. Our results implicate zinc as a major determinant of the ability of the cell to store these other important nutrients.

Zinc is an important structural and/or catalytic cofactor for numerous proteins. For example, it was estimated recently that as many as 10% of the approximately 30,000 different proteins encoded by the human genome require zinc for their function (1). If accumulated in excessive amounts, however, zinc can also be toxic to cells (4). Thus, organisms have evolved with homeostatic mechanisms to maintain a relatively constant intracellular environment in the face of changing levels of extracellular zinc. One primary mechanism of zinc homeostasis is the control of zinc uptake across the plasma membrane (11). In addition, sequestration of zinc within intracellular organelles is an important strategy of zinc homeostasis. Organellar zinc sequestration is clearly needed for zinc homeostasis in fungi and plants and may also be a component of mammalian zinc homeostasis (3, 8, 10, 20, 22, 33, 34, 37, 41).

In the yeast *Saccharomyces cerevisiae*, approximately 1.5×10^7 total zinc atoms per cell are required for optimal growth (34). This value is referred to as the "zinc quota" for yeast and probably represents the level required to optimally metalate zinc-dependent proteins in the cell (40). Below that amount, cells grow more slowly. When zinc levels drop below a mini-

mum threshold of $\sim 5 \times 10^6$ atoms per cell, growth ceases altogether. Our previous results have shown that the Zap1 transcription factor helps maintain intracellular zinc levels for growth by regulating several genes in response to zinc deficiency (32, 52). These genes include the *ZRT1*, *ZRT2*, and *FET4* genes encoding zinc uptake transporters on the plasma membrane (47, 50, 51). Increased expression of these genes increases the zinc uptake capacity of the cell more than 100-fold.

Previous studies have implicated the vacuole of yeast as a major site of zinc sequestration in the cell, and the level of zinc in the vacuole is also controlled by Zap1 (5, 20, 34, 48). Two transporters, Zrc1 and Cot1, are responsible for zinc transport into this compartment. Genetic studies of these transporters have indicated three major roles for vacuolar zinc sequestration. First, the vacuole is required for zinc detoxification. When zinc is abundant, the metal is taken up into this compartment, thereby limiting its toxicity. Zrc1 and Cot1 are both required for zinc detoxification. Second, the vacuole provides a site of zinc storage. When cells are zinc replete, Zrc1 and Cot1 mediate zinc accumulation in the vacuole. Under conditions of zinc deficiency, the Zrt3 transporter is up-regulated by Zap1 to mobilize sequestered zinc from that compartment (34). Finally, the vacuole plays an especially important role in the resistance to "zinc shock" (36). Zinc shock occurs when zinc-limited cells are resupplied with zinc. Because zinc-limited cells have such a high capacity for zinc uptake, addition of even modest amounts of zinc results in the accumulation of extremely high concentrations of the metal. The vacuole and the Zrc1 and Cot1 transporters are required for surviving zinc shock.

---

* Corresponding author. Mailing address: Department of Nutritional Sciences, 1415 Linden Drive, University of Wisconsin—Madison, Madison, WI 53706. Phone: (608) 263-1613. Fax: (608) 262-5860. E-mail: deide@wisc.edu.
† Present address: Department of Chemistry, Northwestern University, Evanston, IL 60208-3113.
‡ Supplemental material for this article may be found at http://ec.asm.org/.
▽ Published ahead of print on 25 May 2007.

These genetic studies indicated that vacuolar zinc sequestration was critical for zinc homeostasis. However, several questions remained unanswered. For example, what are the levels of zinc sequestered in the vacuole under various conditions of zinc availability? Second, what is the role of the vacuole in buffering zinc levels in other compartments, such as the cytosol and mitochondria? Third, are there other significant sites of zinc storage elsewhere in the cell? Finally, what is the distribution of other elements in the cell and does zinc status alter those distributions? These important questions were addressed in this study.

MATERIALS AND METHODS

Yeast strains and growth conditions. *S. cerevisiae* strains DY1457 (*MATα ade6 can1 his3 leu2 trp1 ura3*) and CM104 (*MATα ade6 can1 his3 leu2 trp1 ura3 zrc1Δ::HIS3 cot1Δ::URA3*) were used in this study (34). Yeast strains were grown in zinc-replete synthetic defined (SD) medium that contains 6.7 g/liter yeast nitrogen base (Q-BIOgene) plus 2% (wt/vol) glucose and any necessary auxotrophic requirements. This medium contains 0.9 mM Ca, 3.5 mM Cl, 1.2 μM Fe, 7 mM K, 4.1 mM Mg, 1.7 mM Na, 7 mM P, and 2.5 μM Zn. Zinc-limited cells were grown in Chelex-treated synthetic defined (CSD) medium (32) with 2% (wt/vol) glucose and necessary auxotrophic requirements. CSD medium is zinc limiting because zinc was removed from SD medium by pretreatment with Chelex 100 resin (Sigma). The concentration of zinc remaining in CSD medium is less than 100 nM (32), and other divalent cations were added back to their original concentrations. Cells were also grown in low-zinc medium (LZM), which is similar to SD medium but zinc limiting due to the addition of 1 mM EDTA, a strong zinc chelator (16). For steady-state growth experiments, yeast strains were incubated for 20 h with aeration at 30°C in CSD or SD medium supplemented with up to 1,000 μM ZnCl$_2$. SD medium contains a basal zinc concentration of 2.5 μM. For zinc shock experiments, cells were zinc limited by overnight growth in CSD medium, their cell walls were removed to form spheroplasts, and they were then treated with 100 μM ZnCl$_2$. Spheroplasts were used to allow subsequent organelle isolation. Zn treatments were performed in media containing 0.6 M sorbitol to maintain the integrity of the spheroplasts. The cell number per milliliter of culture was determined by measuring the optical density at 600 nm (OD$_{600}$) and comparing with a standard curve. All cells were harvested in mid-log phase (OD$_{600}$ of 0.5 to 1) before being processed for subsequent analysis. Spheroplasts were counted using a hemocytometer.

AAS. Measurements of total cellular zinc accumulation were performed by atomic absorption spectrophotometry (AAS). Cells were harvested by centrifuging for 5 min at 1,000 × g and washed twice in cold 1 mM EDTA and once in cold distilled deionized water to remove surface-bound zinc. Cells were then digested overnight at room temperature in 5 ml 15% H$_2$O$_2$, 40% HNO$_3$ (vol/vol). Acid-digested samples were diluted with distilled deionized water, and zinc content was measured using a Perkin Elmer 2800 atomic absorption spectrophotometer.

Isolation of vacuoles and mitochondria. Spheroplasts for vacuole and mitochondrion isolation were prepared using 5 mg Zymolyase 100T (Seikagaku Corporation) per gram of cells (fresh weight) (49). The efficiency of the lysis was determined by AAS analysis of the zinc content of spheroplasts versus that of homogenates of lysed cells. Approximately 50% of total zinc was lost due to incomplete lysis; therefore, to estimate zinc levels in these compartments on a per-cell basis, all measured values for vacuolar and mitochondrial zinc were multiplied by two to account for those losses. Vacuoles were prepared as described previously (42). In brief, spheroplasts were homogenized in 20 ml buffer A (10 mM MES [morpholineethanesulfonic acid]-Tris, pH 6.9, 0.1 mM MgCl$_2$, 12% [wt/vol] Ficoll 400) with a Dounce homogenizer and then centrifuged at 2,200 × g for 10 min. The supernatant was transferred to a polyallomer tube, carefully overlaid with 10 ml buffer A, and centrifuged at 60,000 × g for 30 min in an SW28 rotor. The vacuoles floating on top of the Ficoll were collected, homogenized in 15 ml buffer A, overlaid with 15 ml buffer B (10 mM MES-Tris, pH 6.9, 0.5 mM MgCl$_2$, 8% [wt/vol] Ficoll 400), and then centrifuged at 60,000 × g for 30 min. The vacuoles were again collected, resuspended in 0.2 ml 2× buffer C (10 mM MES-Tris, pH 6.9, 5 mM MgCl$_2$, 25 mM KCl), and stored at −80°C.

Carboxypeptidase Y (CPY) assays were performed to determine the yield of intact vacuoles (29). Vacuoles were incubated in solubilization buffer (10 mM MES-Tris, pH 6.9, 10% [wt/vol] sucrose, 1 mM EDTA, 1% [vol/vol] Triton X-100) on ice for 30 min and then centrifuged for 30 min at 100,000 × g. The supernatant was used for inductively coupled plasma-mass spectrometry (ICP-MS) analyses. Mitochondria were isolated as described by Glick and Pon (17).

Briefly, spheroplasts were homogenized in buffer A (20 mM MES, pH 6.0, 0.6 M sorbitol, 0.5 M phenylmethylsulfonyl fluoride) and centrifuged at 1,500 × g for 5 min. The supernatant was collected and centrifuged at 12,000 × g for 10 min. The pellet was resuspended in 0.2 ml buffer A without phenylmethylsulfonyl fluoride. Five ml of 19% (wt/vol) Nycodenz in buffer A was overlaid with 5 ml of 13.5% (wt/vol) Nycodenz in buffer A. The gradient was overlaid with the crude mitochondrion resuspension and centrifuged at 160,000 × g for 30 min. Mitochondria, appearing as a brown band between the 19% and 13.5% (wt/vol) Nycodenz layers, were collected, resuspended in 20 ml buffer B (20 mM MES, pH 7.4, 0.6 M sorbitol), and centrifuged at 12,000 × g for 10 min. The pellet was resuspended in buffer C and stored at −80°C. The yield of intact mitochondria was determined by activity assays of the matrix enzyme succinate dehydrogenase (39). Aliquots (200 μl) of isolated mitochondria and solubilized vacuoles were digested with 1 volume of 65% HNO$_3$ (vol/vol) at 90°C overnight prior to ICP-MS.

Elemental analysis by ICP-MS. ICP-MS was used to measure Zn levels in isolated organelles. Samples were transferred to Pyrex tubes and digested with 0.5 ml concentrated HNO$_3$ at 110°C for 4 h. Each sample was diluted to 4 to 6 ml with 18 megohm water and analyzed with an Elan DRCe ICP-MS instrument (Perkin Elmer). Methane was used as a collision cell gas to measure iron. Gallium and indium were used as internal standards, added to the digestion acid bottle to a concentration of 20 ppb. National Institute of Standards and Technology traceable single-element ICP standards were used to make up the calibration standards.

Immunoblot analysis. Whole-cell lysates and lysates of isolated organelles were fractionated by sodium dodecyl sulfate-polyacrylamide gel electrophoresis, and immunoblotting was performed using standard protocols (18). A BM chemiluminescence kit (Roche) was used for detection. Antibodies used were mouse anti-CPY, mouse anti-Vma1, mouse anti-Cox2, mouse anti-Dpm1, mouse anti-Pgk1 (all obtained from Molecular Probes), and goat anti-mouse horseradish peroxidase-conjugated secondary antibody (Pierce Chemical Co.).

Cryopreparation and electron probe X-ray microanalysis (EPXMA). The cells were centrifuged for 3 min at 1,800 × g in a Sorvall RT6000B centrifuge. The supernatant was decanted immediately and the pellet prepared for X-ray microanalysis as described in detail in our previous studies (26–28). For cryopreservation, approximately 5 μl of cells from the pellets were rapidly placed on a wooden cryomicrotome specimen stub. The cells on the specimen stub were then plunged into liquid-nitrogen-cooled liquid propane (approximately −185°C) and subsequently stored under liquid nitrogen. The frozen cells from each experiment were sectioned in a cryoultramicrotome (Reichert FCS) at <−160°C and the sections freeze-dried and carbon coated prior to analysis (27).

EPXMA and scanning transmission electron microscopy (STEM) were performed on the freeze-dried cryosections with a transmission electron microscope (JEOL 1200EX TEMSCAN) equipped with a low-background rotation stage (model no. 925; Gatan, Inc., Pleasanton, CA), a scanning device, additional hard X-ray aperture, a collimated 30-mm^2 Si(Li) energy-dispersive X-ray detector (Oxford Instruments America, Palo Alto, CA), and a pulse processor; the scanning and multichannel analyses were conducted with an X-ray pulse processor (4pi Analysis spectral engine; 4pi Analysis, Inc., Durham, NC). Operating parameters and strategies for obtaining quantitative X-ray images were implemented as described extensively elsewhere (19, 25–27). Basically, 128- by 128-pixel spectral data sets were obtained at approximately ×10,000 magnification (1 pixel = 0.2 μm^2) with a beam current of approximately 1 nA and a dwell time of 4 s per pixel, with automation (19) and quantitation (27) carried out as previously described. The elemental contents of whole cells and cell regions (i.e., vacuoles or nonvacuolar cytoplasm) were determined by drawing around, i.e., masking, each cell or individual vacuole present; with this method, the cytoplasmic compartment included all structures except the vacuole, i.e., the endoplasmic reticulum (ER), Golgi body, nucleus, mitochondria, and lysosomes. Zinc associated with cell walls was not detectable. Negative values for concentrations are generally reflective of statistical variations, where a noisy background removal from an elemental peak can sometimes exceed the peak signal alone. Values that were consistently negative over numerous measurements were deemed below the detectable level for that element and are so noted in Tables 1 and 2 (46). Element concentrations in nmol/mg (dry weight) were converted to pmol/10^6 cells by use of dry weights determined from a known number of cells or from purified vacuoles from a known number of cells based on recovery of CPY activity. Those conversion factors were 0.09 mg (total dry weight) per 10^6 whole cells and 0.02 mg (vacuole dry weight) per 10^6 cells.

Statistical analyses. EPXMA data were obtained from 17 to 76 cells for whole-cell measurements, 12 to 44 cells for vacuole measurements, and 17 to 43 cells for nonvacuolar cytoplasm measurements, depending on the strain and growth condition. Separate statistical analyses were done by compartment (whole cell, vacuole, or nonvacuolar cytoplasm). For each element, effects of

TABLE 1. Effects of zinc status on the accumulation and distribution of zinc[a]

Strain	Treatment	Zn content (nmol/mg [dry wt]) (mean ± SE)			Compartment	P value		
		Whole cell	Vacuole	Cytoplasm		L vs M	M vs H	L vs H
WT	L	ND	1.4 ± 1.7	1.7 ± 1.6	Whole cell	NS	<0.001	<0.005
	M	ND	ND	ND	Vacuole	NS	<0.0001	<0.0001
	H	3.8 ± 0.9	11.9 ± 1.4	0.7 ± 0.9	Cytoplasm	NS	NS	NS
						0 vs 10	10 vs 20	0 vs 20
WT	0	ND	1.4 ± 1.7	1.7 ± 1.6	Whole cell	<0.0001	NS	<0.0001
	10	7.1 ± 1.0	18.6 ± 2.4	1.4 ± 1.2	Vacuole	<0.0001	<0.05	<0.0001
	20	9.2 ± 1.7	36.4 ± 5.3	3.4 ± 1.0	Cytoplasm	NS	NS	NS
zrc1Δ cot1Δ mutant	0	ND	0.2 ± 1.2	ND	Whole cell	<0.0001	<0.01	<0.0001
	10	1.9 ± 0.6	6.5 ± 1.3	0.7 ± 0.9	Vacuole	<0.0001	<0.001	<0.0001
	20	5.6 ± 1.0	13.9 ± 2.6	1.8 ± 0.7	Cytoplasm	NS	NS	NS

[a] The levels of zinc in whole cells, vacuoles, and the nonvacuolar cytoplasm were determined by EPXMA under steady-state (first three rows) and zinc shock (all other rows) conditions. Data were obtained from 17 to 76 cells for whole-cell measurements, 12 to 44 cells for vacuole measurements, and 17 to 43 cells for nonvacuolar cytoplasm measurements, depending on the strain and growth condition. WT, wild type; L, low zinc (CSD medium); M, moderate zinc (SD medium with 0 Zn); H, high zinc (SD medium plus 100 μM Zn); 0, 0 min; 10, 10-min Zn treatment; 20, 10-min Zn treatment plus 20-min chase; ND, not detectable; NS, not significant ($P > 0.05$).

strain and condition and possible interaction were determined using an extension of the Mann-Whitney test to two-factor analysis of variance on ranked data. Post hoc examination of pairs of zinc levels (Tables 1 and 2) under each treatment condition was done using the Mann-Whitney test. Analysis of covariance allowing for differing slopes was performed on the EPXMA data obtained from individual cells, regressing one element on another and adjusting for compartment, strain, and condition as appropriate. The replicate effect was negligible and not further considered. Type III adjusted P values for Fig. 6 and 7 are reported in Results.

RESULTS

Effect of zinc availability on total cellular and organellar zinc levels. To assess the effects of zinc status on cellular zinc accumulation, wild-type cells were grown in media containing a range of zinc concentrations and then assayed for total zinc levels by AAS. zrc1Δ cot1Δ mutant cells were also assayed to determine whether loss of the Zrc1 and Cot1 vacuolar zinc transporters alters zinc accumulation and the distribution of zinc within cells. As shown in Fig. 1A, low levels of total cellular zinc in wild-type cells grown in zinc-deficient CSD medium were measured (17.8 ± 1.6 pmol/10^6 cells). When wild-type cells were grown in untreated SD medium, containing a basal concentration of 2.5 μM Zn, a higher level of total zinc was observed (57.0 ± 3.0 pmol/10^6 cells). With increasing amounts of $ZnCl_2$ added to SD medium, total cellular zinc accumulation also increased. The most dramatic increase was observed when cells were grown in SD medium plus 1,000 μM $ZnCl_2$, suggesting a loss of zinc homeostasis under these high-zinc conditions. Consistent with this conclusion, cell growth is blocked when the metal is added at concentrations greater than 4 mM (36).

zrc1Δ cot1Δ mutant cells also had low total zinc levels when grown in CSD medium (11.1 ± 0.1 pmol/10^6 cells) and increased zinc levels when grown in SD medium supplemented with up to 25 μM $ZnCl_2$. Because of the lack of the vacuolar zinc transporters in this mutant, these cells are unable to tolerate zinc concentrations above 25 μM (36) and therefore could not be assayed at higher concentrations. However, over the range of zinc availability from CSD medium to SD medium plus 25 μM $ZnCl_2$, little difference in total accumulation was

observed between mutant and wild-type cells. Given the role of Zrc1 and Cot1 in transporting zinc into the vacuole, these results indicate that vacuolar sequestration is not a major factor in determining total zinc accumulation over this range of extracellular zinc. An important role for the vacuole at concentrations higher than 25 μM is suggested by the sensitivity of the mutant to increased zinc levels.

Previous studies indicated that zinc can be sequestered in the vacuole, but the actual zinc storage capacity of the vacuole was not determined (34, 36). To assess the effects of zinc status on vacuolar zinc accumulation, intact vacuoles were isolated from cells grown as described above for Fig. 1A. Zinc content was then determined by ICP-MS because this method has a greater sensitivity for zinc than does AAS. Both analytical methods yielded statistically equivalent results for total zinc accumulation (data not shown), demonstrating that values obtained with these two methods can be compared directly. Immunoblot analysis showed that the isolated vacuoles used in this study were not contaminated by the cytosol or other subcellular compartments (see Fig. S1 in the supplemental material). Specifically, the Dpm1 ER protein, the mitochondrial Cox2 protein, and the cytosolic Pgk1 protein were not detected in isolated vacuole preparations. As expected, the Vma1 vacuolar membrane protein and the CPY luminal vacuolar protein were highly enriched in these samples. The vacuolar zinc measurements were normalized based on the recovery of CPY enzymatic activity to quantify the recovery of intact vacuoles.

The effects of zinc status on vacuolar zinc accumulation in wild-type cells were similar to those observed for total zinc levels (Fig. 1B). Vacuolar zinc in CSD medium-grown wild-type cells was 10.4 ± 3.6 pmol/10^6 cells. Increasing extracellular zinc concentrations resulted in markedly elevated vacuolar zinc accumulation. A large increase in zinc accumulation was observed to occur in vacuoles of cells grown with 1,000 μM zinc, consistent with the loss of homeostatic regulation suggested above for total zinc. Consistent with the expected loss of vacuolar zinc transport, zrc1Δ cot1Δ mutants had very low vacuolar zinc levels at all concentrations tested. For example, vacuolar zinc in mutant cells grown in SD medium with no

TABLE 2. Effects of zinc status on the accumulation and distribution of other elements in wild-type cells[a]

Element	Treatment	Element content (nmol/mg [dry wt]) (mean ± SE)			Compartment	P value		
		Whole cell	Vacuole	Cytoplasm		L vs M	M vs H	L vs H
Ca	L	15.8 ± 0.9	28.4 ± 2.0	12.3 ± 0.9	Whole cell	<0.005	<0.0001	NS
	M	12.1 ± 0.9	18.9 ± 2.2	9.9 ± 1.1	Vacuole	<0.001	NS	<0.05
	H	16.8 ± 0.7	23.2 ± 2.1	14.2 ± 0.7	Cytoplasm	NS	<0.0001	NS
Cl	L	62.4 ± 7.7	53.9 ± 7.1	81.7 ± 15.4	Whole cell	NS	<0.0001	<0.0001
	M	68.5 ± 6.6	35.6 ± 4.2	81.8 ± 9.1	Vacuole	<0.05	<0.0001	<0.0001
	H	11.2 ± 0.6	7.8 ± 0.6	12.0 ± 0.6	Cytoplasm	NS	<0.0001	<0.0001
Fe	L	3.0 ± 0.2	2.4 ± 0.1	2.8 ± 0.2	Whole cell	NS	NS	NS
	M	4.2 ± 0.7	3.5 ± 0.9	4.2 ± 1.0	Vacuole	NS	NS	NS
	H	3.1 ± 0.1	2.9 ± 0.1	3.1 ± 0.2	Cytoplasm	NS	NS	NS
K	L	511.6 ± 21.0	266.8 ± 20.6	664.8 ± 23.5	Whole cell	NS	<0.0001	<0.0001
	M	557.1 ± 24.2	539.6 ± 53.3	525.8 ± 26.5	Vacuole	<0.0001	<0.0001	<0.0001
	H	806.9 ± 23.5	752.2 ± 34.9	761.1 ± 33.2	Cytoplasm	<0.005	<0.0001	NS
Mg	L	82.7 ± 9.4	236.4 ± 19.0	42.7 ± 1.9	Whole cell	NS	<0.0001	<0.0001
	M	82.3 ± 8.0	223.3 ± 17.0	46.6 ± 4.6	Vacuole	NS	<0.005	<0.05
	H	150.9 ± 11.2	320.7 ± 18.9	93.5 ± 3.5	Cytoplasm	NS	<0.0001	<0.0001
Na	L	11.7 ± 6.3	16.8 ± 11.9	14.9 ± 13.1	Whole cell	<0.0001	<0.0001	NS
	M	ND	ND	ND	Vacuole	<0.0001	<0.0001	<0.0001
	H	9.8 ± 2.6	37.4 ± 4.3	0.6 ± 2.6	Cytoplasm	<0.0001	<0.0001	NS
P	L	670.4 ± 49.2	1,496.6 ± 68.1	447.9 ± 12.6	Whole cell	NS	<0.0001	<0.0001
	M	645.3 ± 50.9	1,422.8 ± 83.8	449.9 ± 42.9	Vacuole	NS	<0.0001	<0.001
	H	1,084.2 ± 48.6	1,812.7 ± 65.1	830.3 ± 20.4	Cytoplasm	NS	<0.0001	<0.0001
						0 vs 10	10 vs 20	0 vs 20
Ca	0	15.8 ± 0.9	28.4 ± 2.0	12.3 ± 0.9	Whole cell	NS	<0.0001	<0.005
	10	18.1 ± 0.9	20.9 ± 2.2	16.8 ± 1.1	Vacuole	<0.0001	<0.0001	<0.0001
	20	12.4 ± 0.4	12.2 ± 0.5	12.7 ± 0.4	Cytoplasm	<0.005	<0.05	NS
Cl	0	62.4 ± 7.7	53.9 ± 7.1	81.7 ± 15.4	Whole cell	<0.0001	<0.0001	NS
	10	35.5 ± 4.9	29.3 ± 4.2	53.7 ± 9.7	Vacuole	<0.001	NS	<0.005
	20	101.6 ± 16.0	38.6 ± 8.6	93.3 ± 19.1	Cytoplasm	<0.001	<0.01	NS
Fe	0	3.0 ± 0.2	2.4 ± 0.1	2.8 ± 0.2	Whole cell	NS	<0.05	<0.001
	10	2.7 ± 0.1	2.3 ± 0.2	2.9 ± 0.2	Vacuole	NS	NS	NS
	20	2.4 ± 0.2	2.4 ± 0.3	2.1 ± 0.2	Cytoplasm	NS	<0.005	<0.05
K	0	511.6 ± 21.0	266.8 ± 20.6	664.8 ± 23.5	Whole cell	NS	<0.005	<0.005
	10	527.9 ± 19.7	506.6 ± 34.0	507.5 ± 11.8	Vacuole	<0.0001	NS	<0.0001
	20	634.6 ± 31.7	452.1 ± 26.2	680.7 ± 36.0	Cytoplasm	<0.0001	<0.0001	NS
Mg	0	82.7 ± 9.4	236.4 ± 19.0	42.7 ± 1.9	Whole cell	NS	NS	NS
	10	81.2 ± 6.3	196.5 ± 10.7	47.9 ± 2.2	Vacuole	NS	NS	<0.05
	20	71.5 ± 5.5	189.9 ± 9.8	44.8 ± 4.0	Cytoplasm	NS	<0.05	NS
Na	0	11.7 ± 6.3	16.8 ± 11.9	14.9 ± 13.1	Whole cell	NS	<0.001	NS
	10	9.5 ± 4.4	46.9 ± 10.7	2.9 ± 3.6	Vacuole	<0.05	<0.01	<0.0001
	20	16.9 ± 3.6	79.1 ± 12.7	2.1 ± 1.2	Cytoplasm	NS	NS	NS
P	0	670.4 ± 49.2	1,496.6 ± 68.1	447.9 ± 12.6	Whole cell	NS	NS	NS
	10	615.0 ± 35.5	1,274.9 ± 31.9	407.8 ± 11.8	Vacuole	<0.05	NS	<0.005
	20	607.5 ± 40.7	1,240.2 ± 64.2	431.3 ± 41.4	Cytoplasm	NS	NS	<0.05

[a] The levels of the listed elements in whole cells, vacuoles, and the nonvacuolar cytoplasm were determined by EPXMA under steady-state (first set of elements Ca to P) and zinc shock (second set of elements Ca to P) conditions. Data were obtained from 34 to 76 cells for whole-cell measurements, 17 to 44 cells for vacuole measurements, and 17 to 43 cells for nonvacuolar cytoplasm measurements, depending on the growth condition. See footnote *a* of Table 1 for abbreviations.

added zinc was 13.4 ± 3.4 pmol/10[6] cells. These results indicate that no other transporter proteins contribute significantly to vacuolar zinc influx under these steady-state growth conditions.

Zinc accumulation in isolated mitochondria was also assayed. Mitochondria were isolated with their contents intact, as determined by recovery of the matrix enzyme succinate dehydrogenase. While isolated mitochondria were free of detect-
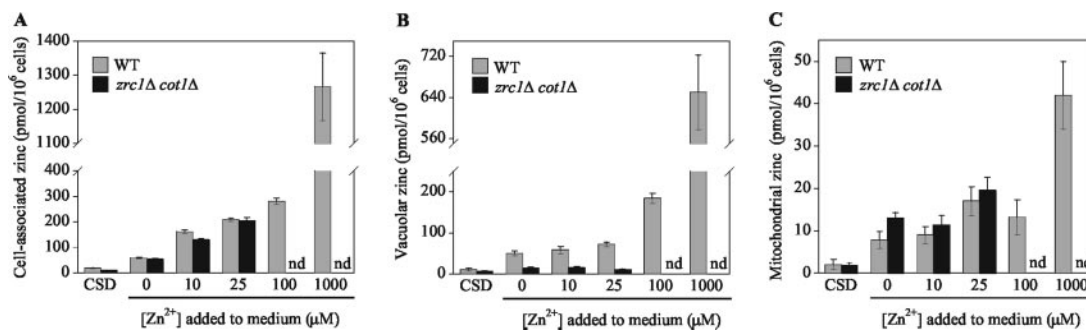
FIG. 1. Effect of zinc status on accumulation and distribution of zinc. Wild-type (WT) and *zrc1Δ cot1Δ* mutant cells were grown in zinc-deficient CSD medium or in SD medium supplemented with the indicated concentrations of $ZnCl_2$. After 20 h, cells were harvested in log phase and assayed for (A) total cell-associated zinc, by AAS, and for (B) vacuolar zinc and (C) mitochondrial zinc, by ICP-MS analysis of isolated organelles. The data reported are the means of at least three independent cultures, and the error bars represent ±1 standard error. nd, not determined (*zrc1Δ cot1Δ* cells are not viable under those conditions of growth).

able vacuolar and cytosolic contamination, some ER membranes, as indicated by detection of Dpm1, copurified with the mitochondria (see Fig. S1 in the supplemental material). Because the contents of the highly reticulated structure of the ER are likely to be lost during cell disruption, we believe that the zinc levels measured in these preparations correspond largely to mitochondrial zinc, although we cannot exclude entirely some contribution of ER zinc. Zinc accumulation in the mitochondrial preparations was much lower than the vacuolar levels. The level of mitochondrial zinc in CSD medium-grown wild-type cells was approximately 1 pmol/10^6 cells and increased to 5 to 10 pmol/10^6 cells in SD medium-grown cells (Fig. 1C). Little change in mitochondrial zinc levels occurred in cells grown with up to 100 μM zinc, suggesting this level was regulated perhaps by mitochondrial zinc import and/or export transporters. A marked increase in zinc was again observed at 1,000 μM, suggesting that this homeostatic control was overwhelmed in these cells.

Compared to the wild type, the *zrc1Δ cot1Δ* mutant showed no significant difference in mitochondrial zinc levels as extracellular concentrations were raised from CSD medium to SD medium containing 25 μM added zinc. Given the absence of vacuolar zinc accumulation observed for the *zrc1Δ cot1Δ* mutant (Fig. 1B), these data indicate that vacuole zinc sequestration does not influence zinc levels in the mitochondria over this range of zinc. In addition, given that total cellular zinc increases for the mutant over this range (Fig. 1A) while mitochondrial zinc does not, we conclude that excess zinc accumulates in another compartment of *zrc1Δ cot1Δ* cells, perhaps the cytosol. Attempts to directly analyze cytosolic zinc by this fractionation method were thwarted by breakage of a large fraction of the vacuoles (>50%) and release of their zinc during cytosol preparation (data not shown).

Analysis of intracellular zinc distribution by EPXMA. An important caveat of the organellar isolation experiments described above is that some zinc may be lost from intact vacuoles and/or mitochondria by transporter-mediated efflux during their isolation. Therefore, the values of zinc measured in these studies may be underestimates of the true in vivo values. To address this issue, an alternative approach to examine the intracellular distribution of metal ions, EPXMA, was used. Wild-type yeast cells were grown under low-zinc (CSD me-

dium), moderate-zinc (SD medium), and high-zinc (SD medium plus 100 μM $ZnCl_2$) conditions and then quickly frozen, cryosectioned, freeze-dried, and analyzed by EPXMA. This method preserves the intracellular distribution of labile elements that can be lost in chemically fixed cells. EPXMA also has the advantage of measuring several different elements (e.g., Ca, Cl, Fe, K, Mg, Na, P, and Zn) in the sample simultaneously. We will first focus on the results obtained for zinc and then consider the effects of changing zinc status on the distribution of other elements later in this report. An example analysis of the distributions of various elements detectable by EPXMA is shown in Fig. 2. Figure 2, left, shows STEM images of several cells grown in either low zinc (CSD medium) (Fig. 2A) or high zinc (SD medium plus 100 μM $ZnCl_2$) (Fig. 2B). Some deformation of these normally spherical cells due to cryosectioning was observed. The other panels show the distributions of Ca, P, and Zn in these cells, represented using a false color temperature scale. Phosphorus and magnesium were used as vacuole markers because these elements are known to accumulate in the vacuole to high levels (2, 24). Total, vacuolar, and nonvacuolar cytoplasmic zinc levels for wild-type cells are reported in Table 1. While these values were below the level of detection in CSD medium- and SD medium-grown cells, zinc was detectable in cells grown in SD medium plus 100 μM $ZnCl_2$. The level of vacuolar zinc in these cells was at least 10-fold greater than the nonvacuolar cytoplasmic level. Thus, in cells grown in SD medium plus 100 μM $ZnCl_2$, the great majority of intracellular zinc is sequestered in the vacuole. In addition, the absolute level of vacuolar zinc is similar to that in isolated vacuoles measured by ICP-MS. When converted to units of zinc per cell, EPXMA indicated that vacuolar zinc in cells grown in SD medium plus 100 μM $ZnCl_2$ was 248 ± 29 pmol/10^6 cells. These results are in close agreement with the data obtained with isolated vacuoles (183 ± 12 pmol/10^6 cells) (Fig. 1B). Zinc levels in *zrc1Δ cot1Δ* mutants were below the level of detection by EPXMA under all growth conditions (data not shown). It should be noted that the sums of the vacuolar and nonvacuolar cytoplasmic zinc levels reported in Table 1 do not equal the whole-cell amount because of slight differences in the dry weights of the compartments with which the values have been normalized.
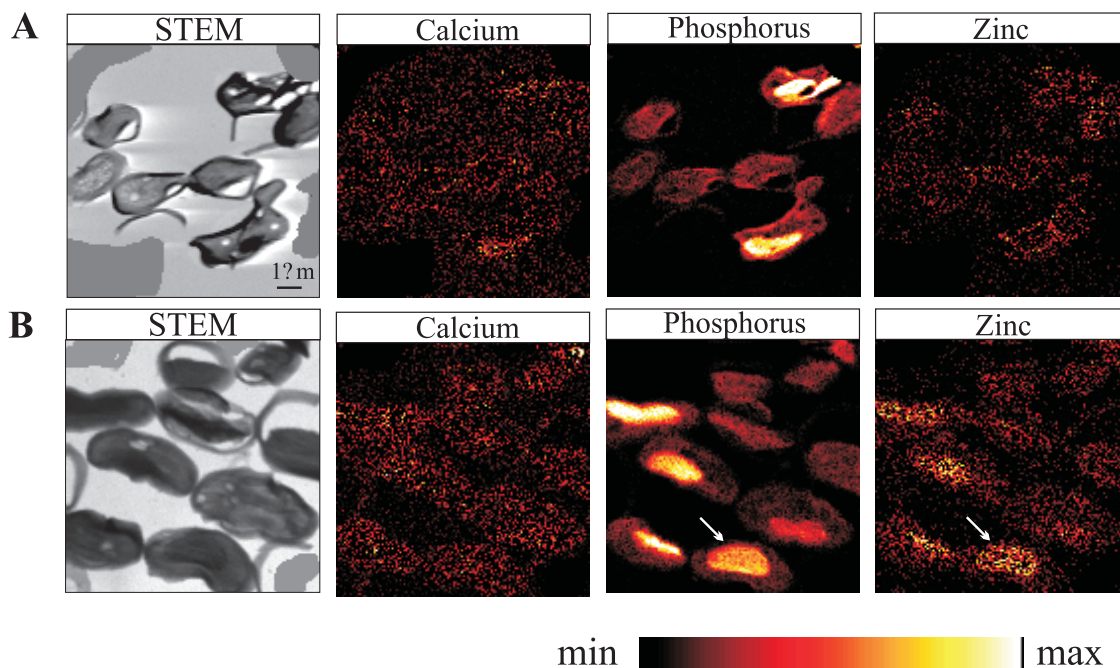
FIG. 2. Analysis of element distribution in cells by EPXMA. Wild-type cells were grown in either (A) zinc-deficient CSD medium or (B) SD medium supplemented with 100 μM $ZnCl_2$. The cells were then cryopreserved, cryosectioned, and analyzed for element distribution by use of EPXMA. The STEM panels show scanning electron micrographs of 0.1-μm-thick sections of several yeast cells. The other panels show energy-dispersive X-ray maps of Ca, P, and Zn from the same sections. These maps are presented as false color images using the scale shown below the cell images. The arrows indicate the vacuole in one of the zinc-treated cells. Note that vacuoles are not apparent in some cells in the field because this compartment was not included in these particular sections of those cells. min, minimum; max, maximum.

Capacity of the vacuolar zinc store to sustain cell growth. The results shown in Fig. 1 and Table 1 indicate that yeast cells grown in high zinc can accumulate a large amount of vacuolar zinc. Based on these data, we estimated that cells grown in SD medium plus 1,000 μM $ZnCl_2$ accumulate as much as 900 pmol vacuolar zinc/10^6 cells. This value corresponds to $\sim 7 \times 10^8$ atoms of vacuolar zinc per cell. Our previous studies indicated that the threshold amount of total intracellular zinc required for cell growth is $\sim 5 \times 10^6$ atoms of zinc per cell (34). Thus, we predicted that high-zinc-grown cells containing an abundant supply of vacuolar zinc could grow for many cell divisions in a medium completely devoid of available extracellular zinc. For example, we predicted that cells grown in SD medium plus 1,000 μM $ZnCl_2$ would contain sufficient intracellular zinc to undergo eight subsequent doublings, i.e., over 200 cells would grow as progeny from a single original zinc-loaded cell. To test this hypothesis, cells were pregrown in SD medium supplemented with different levels of zinc to generate increasing levels of vacuolar zinc stores and then reinoculated into LZM with no added zinc. Without zinc added, LZM contains essentially no bioavailable zinc because of the presence of 1 mM EDTA, a strong zinc chelator. Cell growth, as measured by the optical density of the culture, was monitored over time, and the resulting data were then converted to numbers of population doublings for each condition (Fig. 3A). Wild-type cells grown in SD medium and therefore having relatively low vacuolar zinc underwent only three doublings over a 28-h period in LZM. Three doublings would generate eight progeny cells per initial inoculated cell. Cells pregrown in SD medium plus 25 to 1,000 μM $ZnCl_2$ showed progressively higher growth yields. As

we predicted, cells grown in SD medium plus 1,000 μM $ZnCl_2$ underwent eight doublings of cell number. Several lines of evidence indicate that these effects are due to mobilization of vacuolar zinc stores. First, _zrc1Δ cot1Δ_ mutants grown in SD
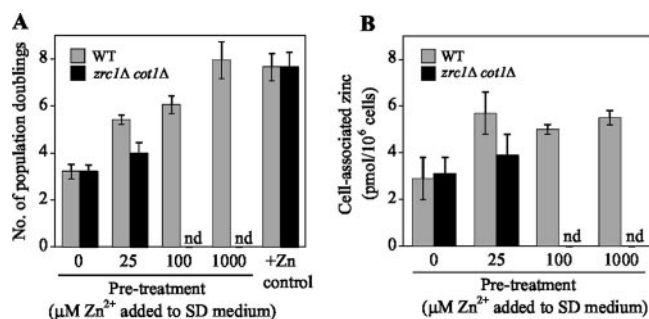

FIG. 3. Effects of the vacuolar zinc store on cell growth under zinc starvation conditions. Wild-type (WT) and _zrc1Δ cot1Δ_ cells were grown overnight in SD medium supplemented with the indicated zinc concentrations. These cells were then washed free of extracellular zinc and inoculated into LZM with no added zinc, i.e., a medium with essentially no bioavailable zinc. (A) Cell densities of the cultures were monitored by measuring the OD_{600} of the cultures after 28 h of incubation. The cell densities were then converted to the numbers of population doublings. Wild-type and mutant cells pregrown in SD medium with no added zinc and then inoculated into LZM plus 100 μM $ZnCl_2$ were used as a control for zinc-replete growth (+Zn control). (B) Total cellular zinc contents of the cells were measured by AAS after 28 h of growth. The data reported are the means of three independent cultures, and the error bars represent ±1 standard error. nd, not determined (_zrc1Δ cot1Δ_ cells are not viable under those conditions of growth).
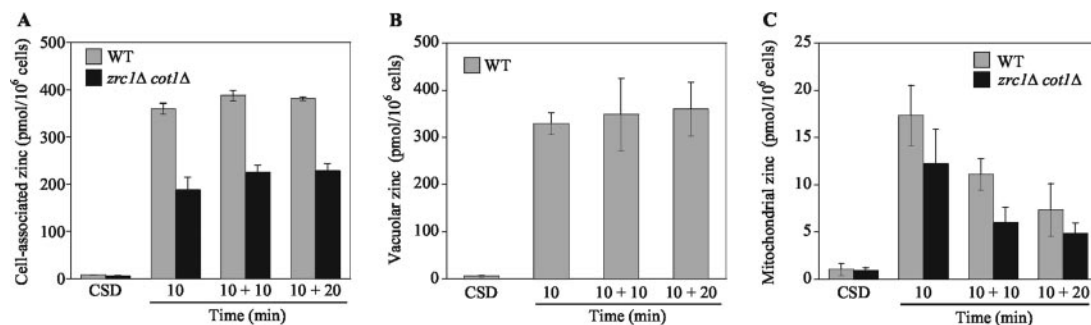
FIG. 4. Effects of zinc shock on the accumulation and intracellular distribution of zinc. (A) Wild-type (WT) and *zrc1Δ cot1Δ* mutant cells were grown in zinc-limiting CSD medium overnight to induce zinc deficiency. The cells were then harvested, and their cell walls were removed to generate spheroplasts; this allowed the rapid isolation of organelles assayed as reported below. To induce zinc shock, 100 μM ZnCl₂ was added to the medium for a 10-min period. After this treatment, the cells were washed free of exogenous zinc and analyzed or incubated for an additional 10-min (10 + 10) or 20-min (10 + 20) chase period without zinc prior to harvesting. Cellular zinc levels were determined using AAS. In addition, vacuoles were isolated from wild-type cells (B), mitochondria were isolated from wild-type and *zrc1Δ cot1Δ* cells (C), and zinc levels were measured by ICP-MS. Vacuoles from *zrc1Δ cot1Δ* cells could not be obtained in this analysis due to organelle fragility; the cause of this fragility is unknown. The data reported are the means of three independent cultures, and the error bars represent ±1 standard error.

medium plus 25 μM ZnCl₂ grew only slightly better than SD medium-grown wild-type or mutant cells. In addition, wild-type and *zrc1Δ cot1Δ* mutant cells grown in SD medium with no added zinc and then inoculated into LZM plus 100 μM ZnCl₂ (Fig. 3A, "+Zn control" columns) also underwent eight doublings during the same period. These results demonstrate the remarkable ability of the vacuolar zinc store to sustain yeast growth for many generations without available extracellular zinc. Following these periods of growth, total cellular zinc levels, as determined by AAS, reached similarly low levels near the minimum level of zinc required for yeast growth (Fig. 3B).

Zinc levels and distribution during zinc shock. Zinc shock occurs when zinc-limited cells are exposed to even modest levels of extracellular zinc. Because zinc-limited cells up-regulate their plasma membrane zinc transporters, newly added zinc can accumulate to very high levels in these cells. Our previous results indicated that the vacuole is required for cells to survive zinc shock (36). To assess the levels and intracellular distributions of zinc during zinc shock, we first used a pulse-chase protocol in conjunction with organelle isolation and AAS/ICP-MS analysis. Cells were zinc limited by growth in CSD medium, their cell walls were removed to form spheroplasts, and they were then treated with 100 μM ZnCl₂. Spheroplasts were used to allow subsequent organelle isolation; levels of zinc accumulation were similar in intact cells and spheroplasts (data not shown). After 10 min, the cells were harvested by centrifugation and analyzed for cellular zinc accumulation by AAS. Alternatively, the zinc-treated cells were resuspended in low-zinc CSD medium and incubated for an additional 10 or 20 min prior to harvesting. Both the wild type and the *zrc1Δ cot1Δ* mutants accumulated considerable zinc during the 10-min pulse, and this zinc was retained during the 20-min chase period (Fig. 4A). *zrc1Δ cot1Δ* mutant cells accumulated ~40% less zinc than wild-type cells, presumably because of the lack of vacuolar sequestration.

To examine vacuolar zinc accumulation, the cells were harvested after the initial zinc pulse and after the chase periods and vacuoles were isolated. We were unable to test *zrc1Δ cot1Δ* mutants in this way because their vacuoles were difficult to isolate following zinc shock due to organelle breakage. No

differences in vacuole morphology were observed, and the cause of this vacuolar fragility in *zrc1Δ cot1Δ* cells is not yet known. Zinc accumulation in wild-type vacuoles was similar to the total zinc accumulation, indicating that most of the zinc accumulated during this treatment was sequestered in the vacuole (Fig. 4B). Finally, mitochondrial zinc levels were examined in zinc-shocked wild-type and *zrc1Δ cot1Δ* cells (Fig. 4C). Mitochondrial zinc levels in both strains rose rapidly and then decreased during the 20-min chase period. ICP-MS analysis indicated that there was no change in mitochondrial Ca levels during zinc shock, suggesting that the observed changes in zinc were not simply due to different degrees of cation leakage from the mitochondria during their preparation (data not shown). Thus, these data further support the hypothesis that mitochondria have mechanisms to maintain zinc homeostasis.

Analysis of zinc shock by EPXMA. EPXMA was also used to examine zinc distribution during zinc shock, and these data are reported in Table 1. Consistent with the AAS/ICP-MS data, total cellular zinc rose to a high level in wild-type cells during zinc shock. Also consistent with these data, wild-type vacuolar zinc increased to a high level. Nonvacuolar cytoplasmic zinc levels remained low relative to vacuolar levels, but an increase in zinc content was detected. This observation confirms that the level of zinc in nonvacuolar compartments does increase during zinc shock.

EPXMA of *zrc1Δ cot1Δ* mutants during zinc shock also detected large increases in total zinc levels. Surprisingly, rapid vacuolar accumulation of high levels of zinc, albeit to a lower level than that observed for the wild type, was also seen in *zrc1Δ cot1Δ* mutant cells. This result indicates that, although Zrc1 and Cot1 are important for zinc influx into the vacuole, other transporters also participate in this process under zinc shock conditions. The identity of those other systems is not yet known.

Effects of zinc status on other elements. EPXMA allows the simultaneous analysis of several elements in addition to zinc. Therefore, we used this method to determine whether zinc status alters the level and/or distribution of other elements in yeast. The whole-cell levels of Ca, Cl, Fe, K, Mg, and P measured by EPXMA in wild-type cells grown in SD medium are
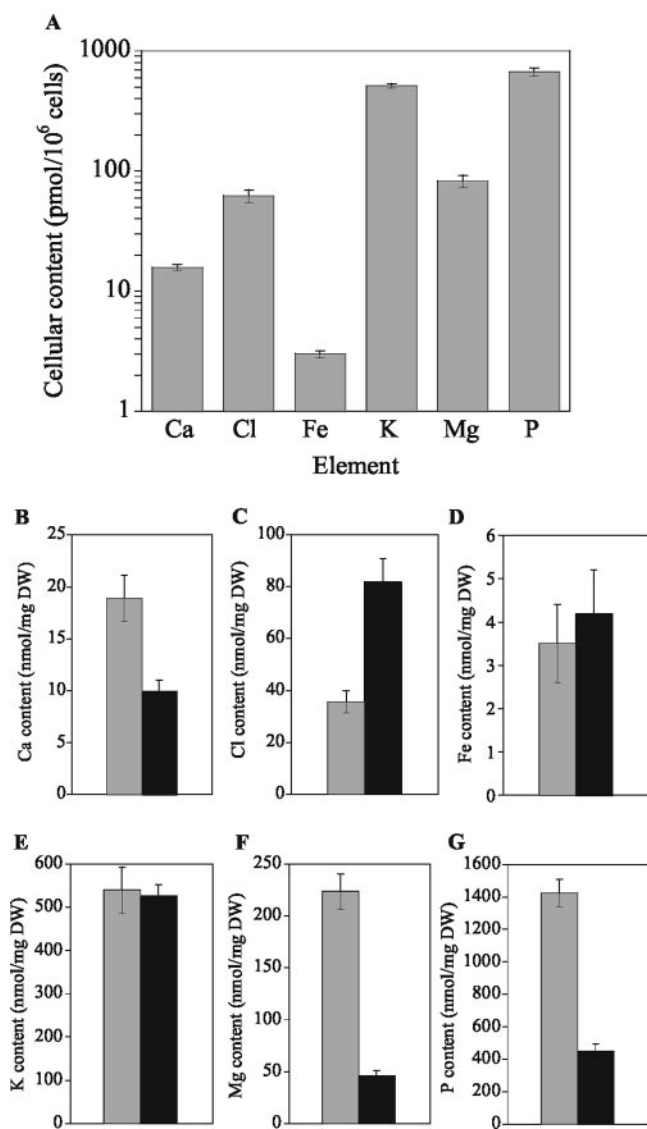
FIG. 5. Element distribution in wild-type cells. Wild-type cells were grown in SD medium without additional zinc for 20 h and harvested in log phase. The cells were then cryopreserved and analyzed for element distribution by use of EPXMA. Energy-dispersive X-ray maps were analyzed, and concentrations of different elements (Ca, Cl, Fe, K, Mg, and P) in (A) whole cells and in (B to G) vacuoles (gray columns) and nonvacuolar cytoplasm (black columns) were determined. The means are reported, and the error bars indicate ± 1 standard error. DW, dry weight.

shown in Fig. 5A. The abundances of P and K were ~10-fold greater than those of Mg and Cl, which in turn were greater than the levels of Ca and Fe. These results are consistent with measurements of these elements in yeast cells as determined by other methods, e.g., ICP-atomic emission spectroscopy (12). Na levels were below the level of detection in cells grown under these conditions. In Fig. 5B to G, the abundances of each element measured in vacuoles and in the nonvacuolar cytoplasmic regions of the cell are plotted. Ca, Mg, and P were found at higher concentrations in the vacuole than in the cytoplasm, while Fe and K were more equally distributed. Cl

was more abundant in the nonvacuolar cytoplasm than within vacuoles.

The data reported in Fig. 5 were obtained from cells grown under moderate-zinc conditions (i.e., SD medium with no additional zinc). The effects of zinc status on these various elements under steady-state growth conditions are reported in Table 2. Total, vacuolar, and nonvacuolar cytoplasmic Fe levels were unaffected by changes in zinc status. Ca and Na levels fluctuated in response to zinc, with levels (i) decreased in SD medium-grown cells versus CSD medium-grown cells and (ii) similar in cells grown in CSD medium and cells grown in SD medium plus 100 μM ZnCl$_2$. Cl levels decreased markedly in all compartments in high zinc. K, Mg, and P all showed statistically significant increased accumulation in response to zinc. For K, this increase was largely due to changes in vacuolar levels and was observed in both SD medium-grown cells and cells grown in SD medium plus 100 μM ZnCl$_2$ relative to CSD medium-grown cells. In contrast, large increases in both vacuolar and cytoplasmic Mg and P were observed. These increases were seen only in cells grown in SD medium plus 100 μM ZnCl$_2$, indicating that this effect is a response to high zinc levels.

To determine if the effects of zinc on the accumulation of these elements were rapid or required long-term incubation under specific zinc conditions, we measured the effects of zinc shock on abundance of these elements (Table 2). Consistent with the increase in K with elevated zinc under steady-state conditions, vacuolar K levels increased twofold following 10 min of zinc shock and remained elevated over the 20-min chase period. A statistically significant increase in total cellular K was detected following the 20-min chase period. Thus, the response of K to increasing zinc occurs very rapidly. In contrast, no increase in Mg or P levels was observed over the zinc shock treatment period. Thus, while the effects of zinc on K levels are rapid, the effects of zinc on Mg and P accumulation require longer periods of incubation in high zinc to occur. Zinc shock caused a decrease in vacuolar Ca and a transient rise in cytoplasmic Ca. Following the chase period, cytoplasmic Ca levels returned to the starting level but vacuolar Ca levels were reduced further. Zinc shock also caused a transient decrease in cellular Cl, followed by an increase that occurred during the chase period. This result indicated that the effect of zinc status on Cl observed under steady-state growth conditions also requires a longer period of incubation to occur. Finally, zinc shock was associated with a fivefold increase in vacuolar Na levels whereas total Na levels were not significantly affected. This result suggests a redistribution of cellular Na into the vacuole along with zinc.

EPXMA data were also collected from *zrc1Δ cot1Δ* mutants grown under steady-state conditions of increasing zinc or following zinc shock. These data are provided in Table S1 in the supplemental material.

The EPXMA data indicated that cellular K, Mg, and P levels rise in response to increased zinc availability under steady-state conditions. To further investigate the correlation between these elements, we plotted those data as scatter plots displaying the results obtained with individual cells. Remarkably, there was a strong positive correlation between Mg and P levels in single cells (Fig. 6). This effect was seen under all treatment conditions and in all compartments ($P < 0.0001$). In
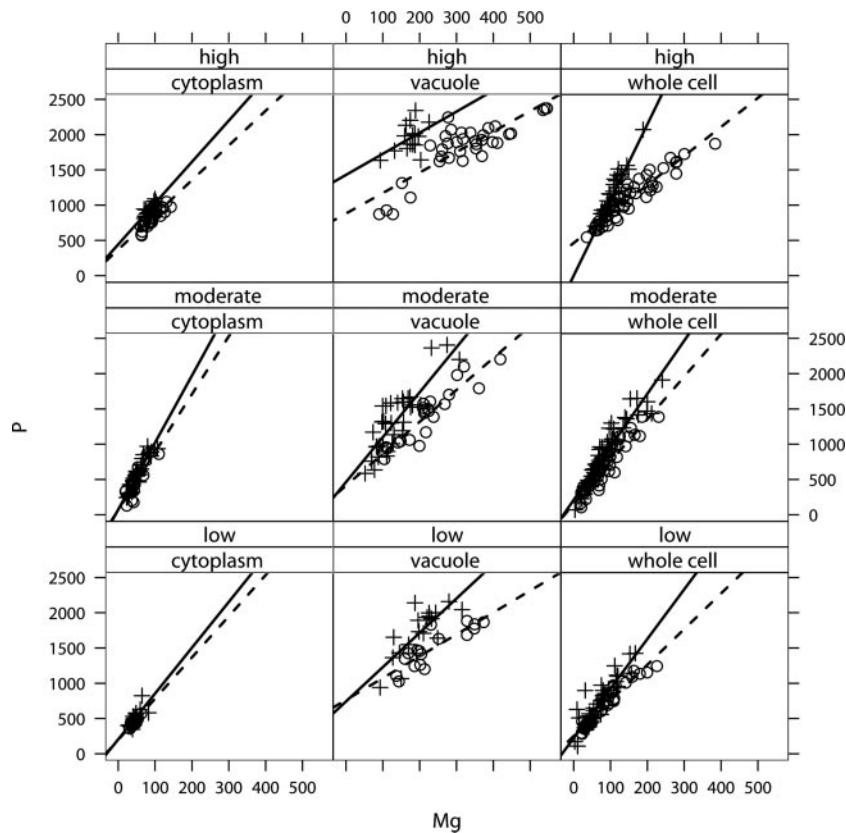
FIG. 6. Correlation between Mg and P contents in individual cells. Nonvacuolar cytoplasmic, vacuolar, and whole-cell levels of Mg and P, measured in individual cells grown in low (CSD medium), moderate (SD medium), and high (SD medium plus 100 μM ZnCl$_2$) zinc, are plotted. Wild-type values are indicated with circles, and *zrc1Δ cot1Δ* mutant values are indicated with "+" symbols. All values are in nmol/mg (dry weight).

addition, these correlations were observed to occur in *zrc1Δ cot1Δ* mutant cells, although these mutations did alter the slope of the correlation in whole cells under some conditions ($P < 0.05$). These results indicate the strong interdependency of intracellular Mg and P in both wild-type and *zrc1Δ cot1Δ* mutant cells.

To assess the effect of zinc status on the correlation between Mg and P, scatter plots comparing Zn with Mg and Zn with P were prepared (Fig. 7). Figure 7 displays the data for wild-type cells grown in high zinc because this was the only steady-state condition where zinc was detectable by EPXMA. Strong positive correlations between Mg and Zn and between P and Zn were found ($P < 0.0001$). In contrast, there was no clear correlation between Zn and K either in whole cells or in vacuoles ($P > 0.3$) (Fig. 7). In addition, no consistent correlation between K and Mg or between K and P was observed (data not shown).

DISCUSSION

The yeast vacuole is a major storage site for many metabolites and ions, including amino acids, phosphate, and magnesium (23). A major goal of this study was to determine the level to which zinc can be stored in this compartment. Analyses of purified vacuoles and of vacuoles in situ within cells by EPXMA both demonstrated that remarkably high amounts of zinc are stored in the vacuole under conditions of zinc excess.

Under high-zinc conditions, we found that as much as 900 pmol Zn/10^6 cells could accumulate in the vacuole. Under zinc shock conditions, a similarly high amount of zinc (i.e., 758 ± 110 pmol/10^6 cells, as determined by EPXMA) accumulated in this compartment. These levels translate into concentrations of almost 100 mM. We suspect that this concentration is near the maximum storage capacity of the organelle, given that yeast cannot tolerate much higher zinc treatment conditions.

In other terms, vacuolar zinc can be as high as 7×10^8 atoms per cell. Given that the minimum amount of zinc required for yeast growth is $\sim 5 \times 10^6$ atoms per cell (34), the vacuolar zinc store can be sufficient to supply this nutrient to many subsequent generations of yeast following transfer from zinc-replete to zinc-limiting media. Given that free-living microbes often face major changes in nutrient availability, the capacities of yeast cells to store zinc and later utilize stored zinc are likely to be of great advantage to these cells growing in the wild. Similarly, vacuolar zinc storage is likely to be an important factor in the successful colonization of host organisms by pathogenic fungi, given that one host response to infection is to withhold zinc from the pathogen (30, 31).

It remains to be determined what factors, aside from the vacuolar zinc transporters themselves, influence the ability of the vacuole to accumulate zinc. One contributing factor is likely to be acidification of that compartment by the vacuolar V-type H$^+$-ATPase. Vacuolar acidification provides the pro-
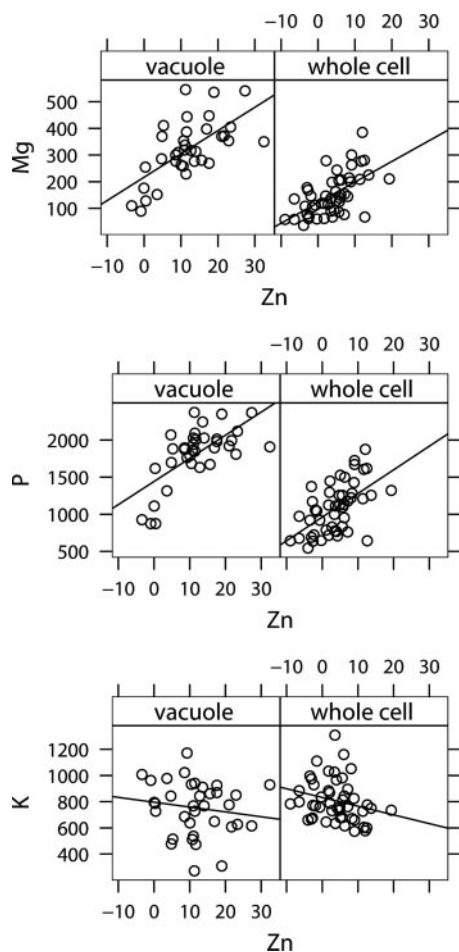
FIG. 7. Correlation between Mg, P, and K contents versus Zn content in individual cells. Vacuole and whole-cell levels of Mg, P, K, and Zn, measured in individual wild-type cells grown in high zinc (SD medium plus 100 μM ZnCl₂), are plotted. All values are in nmol/mg (dry weight).

ton gradient required for zinc uptake into the vacuole via Zrc1 (35). In addition, zinc-binding ligands within the vacuole may contribute to the vacuolar zinc storage capacity. Polyphosphate, i.e., long chains of multiple phosphate groups, accumulates to high levels in the yeast vacuole (24) and can bind zinc with high affinity (2, 38). In addition, organic anions, such as glutamate and citrate, accumulate to high levels in the vacuole (21). A recent study of other fungal species grown under high-zinc conditions indicated that intracellular (and therefore mostly vacuolar) zinc is bound to a mixture of carboxylate and phosphate ligands (13). Similarly, stored zinc in *Arabidopsis halleri*, a zinc-hyperaccumulating plant species, was found complexed with malate, citrate, and phosphate (43). We have examined the importance of polyphosphate to vacuolar zinc storage by use of both nutritional and genetic means to disrupt polyphosphate synthesis and found no effect on zinc storage (C. Simm, unpublished results). Therefore, we conclude that if polyphosphate does contribute to zinc storage, it serves only a minor or perhaps a redundant role with other vacuolar zinc-binding ligands.

A second goal of this study was to determine if the cytosol or

other organelles in the cell represent major sites of zinc storage. For example, it has recently been proposed that the mitochondria of neuronal cells could be a site of zinc storage (44, 45). Our results argue against there being substantial mitochondrial zinc storage in yeast. In addition, we found some evidence for homeostatic regulation of mitochondrial zinc levels in response to variations in zinc availability. For example, during zinc shock, mitochondrial levels rose following a 10-min zinc pulse and then dropped substantially following a 20-min chase period (Fig. 4C). While the components of zinc influx and efflux from mitochondria remain to be identified, we believe that the homeostatic control of mitochondrial zinc is important for cell survival in high zinc. Analogously, several studies have suggested that high mitochondrial zinc levels can inhibit mammalian cell growth (6, 7, 14).

Another potential storage site for zinc in cells is zinc-enriched cytoplasmic vesicles known as "zincosomes." Studies using zinc-sensitive fluorophores, such as Zinquin, have detected labile zinc in such vesicles in many different mammalian cell types (3, 10, 22, 41). Recent studies of yeast carried out using Zinquin detected analogous vesicles that were distinct from vacuoles and mitochondria (9, 11). Nonetheless, while zincosomes may contribute to zinc homeostasis in some important way, e.g., perhaps in the transient movement of free zinc ions, our EPXMA studies demonstrate that these and other compartments in the nonvacuolar cytoplasmic region of yeast cells do not serve as major sites of zinc sequestration relative to the vacuole in zinc-treated cells.

Our previous results implicated Zrc1 and Cot1 as the only zinc transporters responsible for zinc uptake into the vacuole (34). These conclusions were supported here in experiments where cells were grown under steady-state conditions; vacuolar zinc accumulation under these conditions was blocked effectively by mutational inactivation of Zrc1 and Cot1. Surprisingly, however, we found that during zinc shock additional pathways for zinc entry into this organelle exist. Following 10 min of zinc shock, while wild-type cells accumulated 18.6 ± 2.4 nmol Zn/mg (dry weight) in the vacuole, *zrc1Δ cot1Δ* mutants accumulated a lower but still significant amount of vacuolar zinc (6.5 ± 1.3 nmol Zn/mg [dry weight]). These results suggest that additional, albeit less efficient, transporters are present in the vacuolar membrane to mediate zinc import during zinc shock. These transporters may have lower affinity for zinc, and this characteristic would explain why they do not contribute to vacuolar zinc import under steady-state conditions.

A third goal of this study was to determine the importance of vacuole zinc sequestration in buffering the levels of zinc in other compartments. With respect to the mitochondria, we found no such role. Over the testable range of zinc levels, mitochondrial zinc accumulation was unaffected by mutation of the Zrc1 and Cot1 vacuolar zinc transporters. This resistance of the mitochondria to perturbations of cellular zinc homeostasis may be due to the mechanisms in place to maintain mitochondrial zinc homeostasis, as described above. Our ICP-MS results do suggest, however, that the vacuole buffers the zinc levels in other compartments of the cell. When grown in SD medium plus 0 to 25 μM ZnCl₂, *zrc1Δ cot1Δ* mutant cells accumulated as much total zinc as wild-type cells. However, while the wild-type cells put much of that zinc into the vacuole, the *zrc1Δ cot1Δ* mutant did not. Therefore, excess zinc must

accumulate in some other compartment of these mutant cells, perhaps the cytosol, zincosomes, or organelles of the secretory pathway.

Finally, we have focused this study mainly on the role of the yeast vacuole as a subcellular storage and distribution site for zinc. It should be noted that the EPXMA and ICP-MS methodologies used measure both free and bound ions/elements; cell homeostasis likely encompasses concomitant interactions of zinc and other elements in both physiological states. That being said, it was intriguing to find that the levels of K, Mg, and P all rise with increased zinc status. In the case of Mg and P, there was a strong correlation between the levels of these elements in individual cells. Phosphorus accumulation is known to affect Mg uptake, and this effect is thought to be due to differences in vacuolar polyphosphate levels (2). However, we found that the correlation between P and Mg also existed in the nonvacuolar cytoplasmic regions of cells. While most polyphosphate accumulates in the vacuole in yeast, some may also accumulate in other compartments (24). Therefore, this extravacuolar pool of polyphosphate may play a role in determining Mg storage elsewhere in the cell. More surprising is the observation that Zn status correlates closely with both P and Mg. Given that P levels appear to determine, at least in part, cellular Mg levels, we suggest that Zn status somehow alters Mg levels indirectly by affecting P levels. How this occurs remains unclear. What is clear is that the effects of Zn on P and Mg accumulation are not determined by the vacuolar pool of zinc; the same effects were also observed in $zrc1\Delta$ $cot1\Delta$ mutants, in which vacuolar zinc levels are very low. A recent study has shown that polyphosphate accumulation can be affected by many different processes, including ATP generation and primary metabolism (15). We suggest that zinc status affects P through one or more of these indirect mechanisms. Although K levels also increased in response to zinc, several observations indicate that this effect is unrelated to the effects of Zn on Mg and P levels. First, the effects of zinc on K are mostly vacuolar whereas Mg and P are also affected in the cytoplasm. Second, the effects of Zn on K levels were seen during zinc shock while no rapid increase was observed for Mg and P. Finally, no correlation between K and Mg or P in individual cells was observed. Thus, the mechanisms underlying the effects of zinc status on K accumulation are unrelated to those altering (sub) cellular Mg and P levels. These effects and the potentially important role of Na, for example, in these mechanisms need further examination by use of analytical techniques more sensitive than those used here, such as high spatial resolution secondary ion mass spectrometry imaging in combination with molecular-based methods.

ACKNOWLEDGMENT

REFERENCES

1. **Andreini, C., L. Banci, I. Bertini, and A. Rosato.** 2006. Counting the zinc-proteins encoded in the human genome. J. Proteome Res. **5:**196–201.
2. **Beeler, T., K. Bruce, and T. Dunn.** 1997. Regulation of cellular Mg^{2+} by Saccharomyces cerevisiae. Biochim. Biophys. Acta **1323:**310–318.
3. **Beyersmann, D., and H. Haase.** 2001. Functions of zinc in signaling, proliferation and differentiation of mammalian cells. Biometals **14:**331–341.
4. **Cai, L., X. K. Li, Y. Song, and M. G. Cherian.** 2005. Essentiality, toxicology and chelation therapy of zinc and copper. Curr. Med. Chem. **12:**2753–2763.
5. **Conklin, D. S., M. R. Culbertson, and C. Kung.** 1994. Interactions between gene products involved in divalent cation transport in Saccharomyces cerevisiae. Mol. Gen. Genet. **244:**303–311.
6. **Costello, L. C., and R. B. Franklin.** 1998. Novel role of zinc in the regulation of prostate citrate metabolism and its implications in prostate cancer. Prostate **35:**285–296.
7. **Costello, L. C., Y. Liu, R. B. Franklin, and M. C. Kennedy.** 1997. Zinc inhibition of mitochondrial aconitase and its importance in citrate metabolism of prostate epithelial cells. J. Biol. Chem. **272:**28875–28881.
8. **Desbrosses-Fonrouge, A. G., K. Voigt, A. Schroder, S. Arrivault, S. Thomine, and U. Kramer.** 2005. Arabidopsis thaliana MTP1 is a Zn transporter in the vacuolar membrane which mediates Zn detoxification and drives leaf Zn accumulation. FEBS Lett. **579:**4165–4174.
9. **Devirgiliis, C., C. Murgia, G. Danscher, and G. Perozzi.** 2004. Exchangeable zinc ions transiently accumulate in a vesicular compartment in the yeast Saccharomyces cerevisiae. Biochem. Biophys. Res. Commun. **323:**58–64.
10. **Duffy, J. Y., C. M. Miller, G. L. Rutschilling, G. M. Ridder, M. S. Clegg, C. L. Keen, and G. P. Daston.** 2001. A decrease in intracellular zinc level precedes the detection of early indicators of apoptosis in HL-60 cells. Apoptosis **6:**161–172.
11. **Eide, D. J.** 2006. Zinc transporters and the cellular trafficking of zinc. Biochim. Biophys. Acta **1763:**711–722.
12. **Eide, D. J., S. Clark, T. M. Nair, M. Gehl, M. Gribskov, M. L. Guerinot, and J. F. Harper.** 2005. Characterization of the yeast ionome: a genome-wide analysis of nutrient mineral and trace element homeostasis in Saccharomyces cerevisiae. Genome Biol. **6:**R77.
13. **Fomina, M., J. Charnock, A. D. Bowen, and G. M. Gadd.** 2007. X-ray absorption spectroscopy (XAS) of toxic metal mineral transformations by fungi. Environ. Microbiol. **9:**308–321.
14. **Frazzini, V., E. Rockabrand, E. Mocchegiani, and S. L. Sensi.** 2006. Oxidative stress and brain aging: is zinc the link? Biogerontology **7:**307–314.
15. **Freimoser, F. M., H. C. Hurlimann, C. A. Jakob, T. P. Werner, and N. Amrhein.** 2006. Systematic screening of polyphosphate (poly P) levels in yeast mutant cells reveals strong interdependence with primary metabolism. Genome Biol. **7:**R109.
16. **Gitan, R. S., H. Luo, J. Rodgers, M. Broderius, and D. Eide.** 1998. Zinc-induced inactivation of the yeast ZRT1 zinc transporter occurs through endocytosis and vacuolar degradation. J. Biol. Chem. **273:**28617–28624.
17. **Glick, B. S., and L. A. Pon.** 1995. Isolation of highly purified mitochondria from Saccharomyces cerevisiae. Methods Enzymol. **260:**213–223.
18. **Harlow, E., and D. Lane.** 1988. Antibodies: a laboratory manual. Cold Spring Harbor Press, Cold Spring Harbor, NY.
19. **Ingram, P., J. D. Shelburne, and A. LeFurgey.** 1999. Principles and instrumentation, p. 1–58. In P. Ingram, J. D. Shelburne, V. Roggli, and A. LeFurgey (ed.), Biomedical applications of microprobe analysis. Academic Press, San Diego, CA.
20. **Kamizono, A., M. Nishizawa, Y. Teranishi, K. Murata, and A. Kimura.** 1989. Identification of a gene conferring resistance to zinc and cadmium ions in the yeast Saccharomyces cerevisiae. Mol. Gen. Genet. **219:**161–167.
21. **Kitamoto, K., K. Yoshizawa, Y. Ohsumi, and Y. Anraku.** 1988. Dynamic aspects of vacuolar and cytosolic amino acid pools of Saccharomyces cerevisiae. J. Bacteriol. **170:**2683–2686.
22. **Kleineke, J. W., and I. A. Brand.** 1997. Rapid changes in intracellular Zn^{2+} in rat hepatocytes. J. Pharmacol. Toxicol. Methods **38:**181–187.
23. **Klionsky, D. J., P. K. Herman, and S. D. Emr.** 1990. The fungal vacuole: composition, function, and biogenesis. Microbiol. Rev. **54:**266–292.
24. **Kornberg, A., N. N. Rao, and D. Ault-Riche.** 1999. Inorganic polyphosphate: a molecule of many functions. Annu. Rev. Biochem. **68:**89–125.
25. **Lefurgey, A., S. D. Davilla, D. A. Kopf, J. R. Sommer, and P. Ingram.** 1992. Real-time quantitative elemental analysis and mapping: microchemical imaging in cell physiology. J. Microsc. **165:**191–223.
26. **Lefurgey, A., M. Gannon, J. Blum, and P. Ingram.** 2005. Leishmania donovani amastigotes mobilize organic and inorganic osmolytes during regulatory volume decrease. J. Eukaryot. Microbiol. **52:**277–289.
27. **LeFurgey, A., P. Ingram, and J. J. Blum.** 2001. Compartmental responses to acute osmotic stress in Leishmania major result in rapid loss of Na^+ and Cl. Comp. Biochem. Physiol. **128:**385–394.
28. **LeFurgey, A., P. Ingram, and J. J. Blum.** 1990. Elemental composition of polyphosphate-containing vacuoles and cytoplasm of Leishmania major. Mol. Biochem. Parasitol. **40:**77–86.
29. **Li, L., O. S. Chen, D. McVey Ward, and J. Kaplan.** 2001. CCC1 is a transporter that mediates vacuolar iron storage in yeast. J. Biol. Chem. **276:**29515–29519.
30. **Liuzzi, J. P., L. A. Lichten, S. Rivera, R. K. Blanchard, T. B. Aydemir, M. D. Knutson, T. Ganz, and R. J. Cousins.** 2005. Interleukin-6 regulates the zinc transporter Zip14 in liver and contributes to the hypozincemia of the acute-phase response. Proc. Natl. Acad. Sci. USA **102:**6843–6848.
31. **Lulloff, S. J., B. L. Hahn, and P. G. Sohnle.** 2004. Fungal susceptibility to zinc deprivation. J. Lab. Clin. Med. **144:**208–214.
32. **Lyons, T. J., A. P. Gasch, L. A. Gaither, D. Botstein, P. O. Brown, and D. J. Eide.** 2000. Genome-wide characterization of the Zap1p zinc-responsive regulon in yeast. Proc. Natl. Acad. Sci. USA **97:**7957–7962.

33. **Ma, J. F., D. Ueno, F. J. Zhao, and S. P. McGrath.** 2005. Subcellular localisation of Cd and Zn in the leaves of a Cd-hyperaccumulating ecotype of *Thlaspi caerulescens*. Planta **220:**731–736.

34. **MacDiarmid, C. W., L. A. Gaither, and D. Eide.** 2000. Zinc transporters that regulate vacuolar zinc storage in *Saccharomyces cerevisiae*. EMBO J. **19:**2845–2855.

35. **MacDiarmid, C. W., M. A. Milanick, and D. J. Eide.** 2002. Biochemical properties of vacuolar zinc transport systems of *Saccharomyces cerevisiae*. J. Biol. Chem. **277:**39187–39194.

36. **MacDiarmid, C. W., M. A. Milanick, and D. J. Eide.** 2003. Induction of the *ZRC1* metal tolerance gene in zinc-limited yeast confers resistance to zinc shock. J. Biol. Chem. **278:**15065–15072.

37. **Miyabe, S., S. Izawa, and Y. Inoue.** 2001. Zrc1 is involved in zinc transport system between vacuole and cytosol in *Saccharomyces cerevisiae*. Biochem. Biophys. Res. Commun. **282:**79–83.

38. **Moe, O. A., and S. A. Wiest.** 1977. Determination of stability constants for zinc-pyrophosphate complexes. Anal. Biochem. **71:**73–78.

39. **Munujos, P., J. Coll-Canti, F. Gonzalez-Sastre, and F. J. Gella.** 1993. Assay of succinate dehydrogenase activity by a colorimetric-continuous method using iodonitrotetrazolium chloride as electron acceptor. Anal. Biochem. **212:**506–509.

40. **Outten, C. E., and T. V. O'Halloran.** 2001. Femtomolar sensitivity of metalloregulatory proteins controlling zinc homeostasis. Science **292:**2488–2492.

41. **Palmiter, R. D., T. B. Cole, and S. D. Findley.** 1996. ZnT-2, a mammalian protein that confers resistance to zinc by facilitating vesicular sequestration. EMBO J. **15:**1784–1791.

42. **Roberts, C. J., C. K. Raymond, C. T. Yamashiro, and T. H. Stevens.** 1991. Methods for studying the yeast vacuole. Methods Enzymol. **194:**644–661.

43. **Sarret, G., P. Saumitou-Laprade, V. Bert, O. Proux, J. L. Hazemann, A. Traverse, M. A. Marcus, and A. Manceau.** 2002. Forms of zinc accumulated in the hyperaccumulator *Arabidopsis halleri*. Plant Physiol. **130:**1815–1826.

44. **Sensi, S. L., D. Ton-That, P. G. Sullivan, E. A. Jonas, K. R. Gee, L. K. Kaczmarek, and J. H. Weiss.** 2003. Modulation of mitochondrial function by endogenous Zn^{2+} pools. Proc. Natl. Acad. Sci. USA **100:**6157–6162.

45. **Sensi, S. L., D. Ton-That, J. H. Weiss, A. Rothe, and K. R. Gee.** 2003. A new mitochondrial fluorescent zinc sensor. Cell Calcium **34:**281–284.

46. **Warley, A.** 1997. X-ray microanalysis for biologists, p. 227–229. Portland Press, London, United Kingdom.

47. **Waters, B. M., and D. J. Eide.** 2002. Combinatorial control of yeast *FET4* gene expression in response to iron, zinc, and oxygen. J. Biol. Chem. **277:**33749–33757.

48. **White, C., and G. M. Gadd.** 1987. The uptake and cellular distribution of zinc in *Saccharomyces cerevisiae*. J. Gen. Microbiol. **133:**727–737.

49. **Yaffe, M. P.** 1991. Analysis of mitochondrial function and assembly. Methods Enzymol. **194:**627–643.

50. **Zhao, H., and D. Eide.** 1996. The yeast *ZRT1* gene encodes the zinc transporter protein of a high-affinity uptake system induced by zinc limitation. Proc. Natl. Acad. Sci. USA **93:**2454–2458.

51. **Zhao, H., and D. Eide.** 1996. The *ZRT2* gene encodes the low affinity zinc transporter in *Saccharomyces cerevisiae*. J. Biol. Chem. **271:**23203–23210.

52. **Zhao, H., and D. J. Eide.** 1997. Zap1p, a metalloregulatory protein involved in zinc-responsive transcriptional regulation in *Saccharomyces cerevisiae*. Mol. Cell. Biol. **17:**5044–5052.